Design Optimisation of a 6-RSS Parallel Manipulator via Surrogate Modelling

IOP Conf. Series: Materials Science and Engineering **501** (2019) 012020 doi:10.1088/1757-899X/501/1/012020

Design Optimisation of a 6-RSS Parallel Manipulator via Surrogate Modelling

Kantapon Tanakitkorn*

Faculty of International Maritime Studies, Kasetsart University, Si-Racha, Chonburi, 20230, Thailand

* Corresponding Author: kantapon.ta@ku.th

Abstract. Parallel manipulators are robots with the capability to perform motion up to six degrees of freedom. This work presents a surrogate-based optimisation process for designing a 6-RSS parallel manipulator that is driven by six rotary actuators; the kinematic performance of the manipulator is defined by the volume of the total orientation workspace and the global conditioning index. The surrogate modelling technique was demonstrated by simulation to be highly beneficial in exploring the design landscape thoroughly even for a high-dimensional case with six design variables. Computational expense in the optimisation process was reduced by sequentially searching the surrogate models instead of the original performance indices. One platform geometry with the best compromise between the two contradicting indices was obtained in accordance with the weighted-sum function. Despite the fact that this work considers a small-scale 6-RSS parallel manipulator, the presented surrogate-based optimal design framework is generic and can be applied to different types of manipulators.

1. Introduction

Parallel manipulators (PMs) are robots with several closed-kinematic chains of actuators that are connected to the same rigid body. These robots have several advantages over their serial counterparts, such as better load-carrying capacity, higher rigidity, and higher positioning accuracy [1, 2]. This work consider a 6-RSS type manipulator whose base plate and mobile plate are connected by six identical link chains; each chain consists of a revolute actuator (R) and two spherical joints (SS) [3].

Due to the revolute actuation, the platform could create more nonlinear effects to the kinematic chain when compared to the conventional prismatic actuation ones. This problem was addressed by [4], and a kinematic model of a 6-RSS manipulator was analysed for improving quality of trajectory tracking control. A closed-form dynamic equations of 6-RSS manipulators was derived by [5] to take into account the effect of inertia as well as the external forces on the platform. In spite of the nonlinearity, the platforms with rotary actuators have been proven to be practically useful for highspeed manipulation [6].

Regarding the classical optimal design methodologies, different design criteria are considered as objective functions for establishing the best platform design. Performance of different optimisation algorithms were compared and discussed in [7]. The concept of Pareto efficiency may be applied when multiple design criteria are considered simultaneously [8]. A workspace analysis is the primary consideration in a platform design since PMs have relatively small and irregular-shaped workspaces when compared to serial manipulators. The workspace of a manipulator may be identified numerically by discretising the Cartesian space into a finite number of small grids; each grid is checked against a

number of criteria, e.g. that grid is reachable and the joint limits are not violated, and the workspace is formed by connecting all the valid grids together [9]. In addition, a local conditioning index (LCI) [10] is typically used to gives a measure for how close a particular configuration of the platform is to the singular configuration where the platform loses its stiffness or the kinematic chains degenerate. The overall dexterity over a given workspace is referred to as the global conditioning index (GCI) [8]; this global index is computed numerically by averaging the LCI of the discrete grids over the workspace. For further discussion of various performance indices, please refer to [11].

Although simple in concept, the discretisation method is the most computationally expensive part of the optimisation process. This is the case especially when the total orientation workspace is considered because, for every discrete position, the platform must be evaluated at all orientations in a given range [12]. Such a high computational expense can be alleviated by using surrogate models (SMs) as substitutes for the true objective functions. The approximation models can be based on the simple regression models such as polynomial regression [13], but Kriging surrogates appear to be the most popular choices for design search and optimisation [14, 15]. The preferred search algorithm is then used on the SM to avoid evaluating those expensive objective functions, speeding up the optimisation process.

The main aim of this paper is to present a procedure for establishing the optimal platform design via the surrogate modelling approach. To this end, the relevant parameters for a 6-RSS platform are described in Section 2. Kinematic performance evaluation is defined in Section 3. The surrogate-based optimisation framework is explained in Section 4. This is followed by the results and discussion in Section 5. The conclusions are presented in Section 6.

2. Platform Geometry

The PM currently studied is illustrated in Figure 1. It is designed to consist of standard components, these are: 1) a base plate with a radius of r_b, 2) a mobile plate with a radius of r_m, 3) six identical RC servos mounted to the base plate with horn lengths of l_h, and 4) six identical connecting rods with lengths of l_r (each rod has magnetic ball joints on both ends).

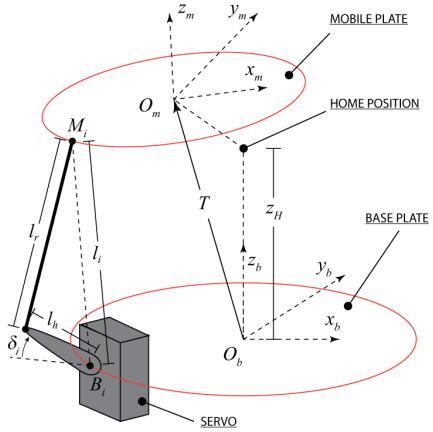

Figure 1. 6-RSS parallel manipulator.

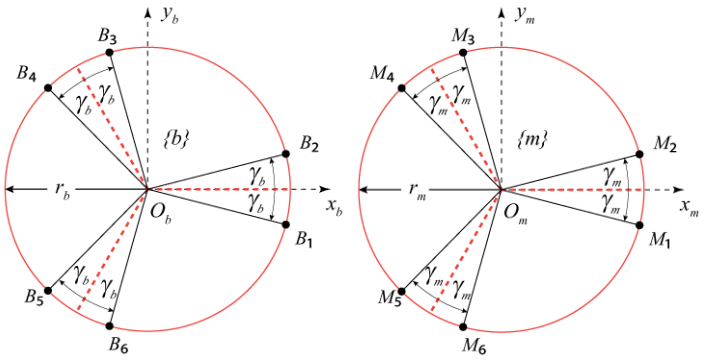

Figure 2. Reference frames that are fixed to the base plate (left) and the mobile plate (right).

Reference frames that are fixed to the centres of the base plate, O_b, and the mobile plate, O_m, are denoted by $\{b\}$ and $\{m\}$, respectively. The joint attachment points on the base plate, B_i, and on the mobile plate, M_i, are grouped into three pairs and are distributed evenly on their respective circles (see Figure 2). Parameters γ_b and γ_m denote the angle spacing between the joints for each pair on the base plate and the mobile plate, respectively.

Joint positions on the base plate expressed in $\{b\}$ for $i = 1,2, \ldots ,6$ are:

$$ {}^{b}B_i = r_b\left[\cos(\Gamma_{b,i}) \quad \sin(\Gamma_{b,i}) \quad 0\right]^{\mathrm{T}}, \tag{1}$$

where

$$\Gamma_{b,i} = [i - 2 - \mathrm{mod}(i, 2)]\frac{\pi}{3} + (-1)^i \gamma_b. \tag{2}$$

Likewise, joint positions on the mobile plate expressed in $\{m\}$ for $i = 1,2, \ldots ,6$ are:

$${}^m M_i = r_m\begin{bmatrix}\cos(\Gamma_{m,i}) & \sin(\Gamma_{m,i}) & 0\end{bmatrix}^\intercal, \tag{3}$$

where

$$\Gamma_{m,i} = [i - 2 - \mathrm{mod}(i, 2)]\frac{\pi}{3} + (-1)^i \gamma_m. \tag{4}$$

The parameter γ_h refers to the angle of the servo horn that is shifted from the radial vector on the base plate; δ_i denotes the angle of the ith servo horn relative to the horizontal plane. For simplicity, a pivot of the ith servo is defined to be coincident with B_i. In this regard, the endpoint of the servo horn expressed in $\{b\}$ is:

$${}^b H_i = {}^b B_i + l_h[\cos(\beta_i)\cos(\delta_i) \quad \sin(\beta_i)\cos(\delta_i) \quad \sin(\delta_i)]^\intercal, \tag{5}$$

where β_i is the angle that the sweeping plane of the ith servo horn makes to the *x-axis* of $\{b\}$:

$$\beta_i = \Gamma_{b,i} - (-1)^i \gamma_h. \tag{6}$$

The mobile plate's configuration (position and orientation) in Cartesian space is converted to an angle for each servo horn in joint space with the following inverse kinematic model [16]:

$$\delta_i = \sin^{-1}\left(\frac{\mathcal{L}}{\sqrt{\mathcal{M}^2 + \mathcal{N}^2}}\right) - \tan^{-1}\left(\frac{\mathcal{N}}{\mathcal{M}}\right), \tag{7}$$

where

$$\mathcal{L} = l_i^2 - l_h^2 + l_r^2, \quad \mathcal{M} = 2l_h(z_{m,i} - z_{b,i}), \quad \text{and} \tag{8}$$
$$\mathcal{N} = 2l_h \sin(\beta_i)(x_{m,i} - x_{b,i}) - 2l_h \cos(\beta_i)(y_{m,i} - y_{b,i}).$$

The parameters $x_{m,i}$ and $x_{b,i}$ denote the x components of ${}^b M_i$ and ${}^b B_i$, respectively, and so forth. Equation (7) is used to verify whether or not the mobile plate is able to attain a certain configuration.

3. Kinematic Performance Evaluation

3.1. Workspace

This paper considers the total orientation workspace, $\mathcal{W}$, that describes how much translational movement is allowed while a parallel robot is still able to perform any orientation in a prescribed set [12]. To identify $\mathcal{W}$, it is necessary to start by discretising the potential range of translational motion with a regular grid; this yields a finite number of positions to be evaluated. Then, each position is tested with the eight representative orientations which are all combination of ± 10 degrees of roll, pitch, and yaw.

A position is said to be a member of $\mathcal{W}$ if all of the eight representative orientations are attainable. The volume of $\mathcal{W}$ is computed by summing the volumes of all the tiny elements. For generality of the analysis, the resulting workspace volume is non-dimensionalised by dividing it by the volume of a sphere of radius r_b.

3.2. Global Conditioning Index

The global conditioning index (GCI) is commonly used for describing the overall performance over the entire workspace [8, 11]:

$$\mathrm{GCI} = \frac{\int_{\mathcal{W}} \kappa(\boldsymbol{J})^{-1} \mathrm{d}\mathcal{W}}{\int_{\mathcal{W}} \mathrm{d}\mathcal{W}} \tag{9}$$

where $\boldsymbol{J}$ is the Jacobian matrix [4] and $\kappa(\boldsymbol{J})$ is the condition number [8]. The total orientation workspace, $\mathcal{W}$, is determined as explained in Section 3.1. A higher GCI means that the platform can be controlled more precisely.

3.3. Mechanism Interference Detection

The feasibility of the design is limited by the interference between the manipulator's parts. To ensure sufficient clearance between the parts, the interference detection algorithm is implemented as follows. On each servo, two fixed-radius circles are assigned to both ends of the servo horn and one circle to the rear part of the servo body. The joints on the mobile plate are also assigned with the circles. The mechanism interference is detected if any of the circle pair intercept, or the servo horns cross. In which case both $\mathcal{W}$ and the GCI are set to zero in order to differentiate the infeasible designs from the feasible ones.

4. Surrogate-Based Design Optimisation

The conventional optimisation methods rely on the direct search of the true objective functions. This framework may not be practical when dealing with expensive objective functions (either computationally or financially or both). However, it is possible to approximate those expensive functions by suitable math functions that are relatively less expensive to evaluate; this approximation is known as surrogate models (SMs) or response surface models (RSMs). The optimisation then performs on the SM to avoid evaluating the expensive objective function.

The surrogate-based optimisation methods involve three stages. First, the true function is sampled at multiple points. This initial data set is used for constructing an SM in the second stage. The search and refine strategy is performed on the SM in the last stage, and it iterates until the solution converges. This procedure is summarised in Figure 3, and the three states are explained in the following subsections.

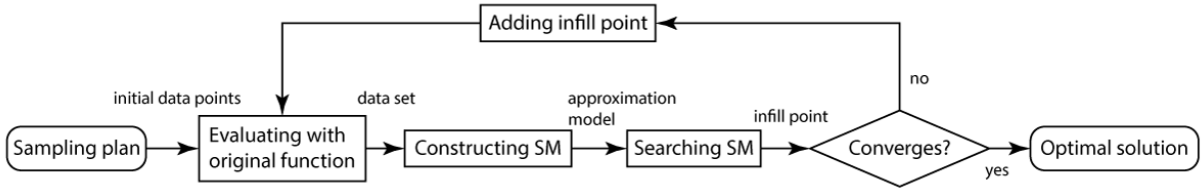

Figure 3. Three fundamental stages of surrogate-based design optimisation.

4.1. Sampling Plan

The surrogate modelling is a process of building an approximation of the original expensive functions. In this regard, like other model fitting tools, an initial set of sample data of an original function is crucial for constructing an SM. The most straightforward way to obtain a *space-filling* data set is to sample the design space evenly and uniformly with the full-factorial sampling plan [17]. Take for instance a 2-dimensional (2D) design space, such a sampling technique will produce a rectangular grid of points. This sampling plan, however, is not efficient because the points overlap when projecting on an axis. Some of these points may be considered repetitive and could be discarded to save computational cost.

Latin hypercube sampling (LHS) is a more efficient alternative that is commonly employed to sample the design space without repetitions. There may be a number of ways to arrange the points in the LHS manner, and in some case the points may bias towards one area. To ensure the data points thoroughly spread over the design space, the minimum distance between all point pairs should be maximised [13]. Since this optimal LHS is *space-filling* and does not generate repetitive points, it allows limited number of samples to gaining as much information of the expensive function as possible.

4.2. Constructing a Surrogate Model

Various types of SMs are presented in the literature. These models are relatively less expensive to evaluate but is sufficiently good in predicting the original function. Kriging is typically the model of choice because it is highly flexible and works well in most situations even with highly-nonlinear, multi-modal functions [18]. Another advantageous of the Kriging model is that it can provide uncertainty estimation of the approximation [13, 14]. This measure is crucial for searching and refining the SM (this point will be discussed in the following subsection).

It has been shown that the platform workspace volume can be improved with a sacrifice of GCI, and vice versa [8]. This means that the ultimate 6-RSS platform design does not exist. Instead, the process will give a range of nondominate designs in the form of a Pareto front [8, 9]; all such designs are valid and optimal but they have different weights for different indices. It is typical, in practice, to combine the two objectives using a weighted-sum function, i.e., $f = w_1 \times f_1 + w_2 \times f_2$, where $w_1 + w_2 = 1$. A Kriging surrogate is then constructed for representing the weighted-sum function that defines the compromise between the two contradict objectives.

4.3. Searching and Refining a Surrogate Model

Once an initial SM has been built, the optimum can be located using one of the existing optimisers such as genetic algorithm (GA). It is important to note that this point is only optimal for the approximation and may not necessarily be so for the true function. In this regard, the point must be considered as an *infill point* which is then evaluated by the original function and augmented into the data set. The SM is refined accordingly and the new optimum is located. By repeating this process, the predicted optimum will converge. The major concern for this pure exploitation infill criterion is that the SM search and refinement will be concentrated on the first optimal region predicted by the SM. As a consequence, the search is highly likely to be trapped in this region, and the global optimum is not guaranteed.

On the other hand, choosing the maximum mean squared error (MSE) as a next infill point will help exploring the uncertain regions of the SM where the global optimum might be hiding [13]. However, this criterion is pure exploration that only yields a more accurate SM. At some point this exploration criterion needs to be stopped and followed by the exploitation search scheme, but at which point can be a tough decision.

Kriging is the Gaussian process-based model that permits the calculation of the expected improvement (EI) [14]. This measure corresponds to the magnitude of improvement expected from refining the SM at any given point. The maximum EI criterion offer a great compromise between exploring uncertain regions and exploiting the current optimum [14, 18]. More importantly, since the points that have been sampled have $\mathrm{EI} = 0$, they will not be sampled again; this implies that the design landscape will be sampled throughout and the global optimum will be found eventually. Using EI as an infill criterion also provides a consistent performance for most situations when compared to other advanced infill criteria [19]. Due to these reasons, the maximum EI infill criterion is considered in this paper.

5. Design Optimisation via Surrogate Modelling

The 6-RSS kinematic model was implemented in MatLab. The surrogate model MatLab toolbox employed in this work is available online at: https://optimizationcodes.wordpress.com. Each platform design was evaluated within a domain of size 0.25m × 0.25m × 0.10m. The domain was discretised with a regular grid. Every position within the domain was tested with the eight representative orientations. Then, the total orientation workspace and the GCI were computed numerically. Supported by Figure 4, a grid size of 2% of the base plate radius is sufficiently small; this setting offers reliable values for both the workspace volume and the GCI with an affordable computing time of just under 360 seconds (obtained with a ThinkPad T450, Intel Core i5-5300U, 8GB RAM) per one platform design.

The surrogate-based optimisation approach was applied for predicting performances of the 6-RSS manipulator over the variation of the six design parameters. The first two were the joint angles on the base plate (γ_b) and the mobile plate (γ_m). Other four more design parameters were as follows: home position (z_H), mobile plate radius (r_m), servo horn's length (l_h) and servo azimuth angle (γ_h). The LHS were used for generating 600 initial samples (100 samples per one design variable). These sample were evaluated in terms of $\mathcal{W}$ and the GCI. The interference detection step was also included in the evaluation to penalise the designs that were mechanically infeasible. For each data point, the two objectives were summed with weights of 0.3 and 0.7 for $\mathcal{W}$ and the GCI, respectively. A Kriging SM of the weighted-sum function were constructed accordingly. More infill points were added by sequentially searching and refining the SM with the GA based on the EI of the weighted-sum function.

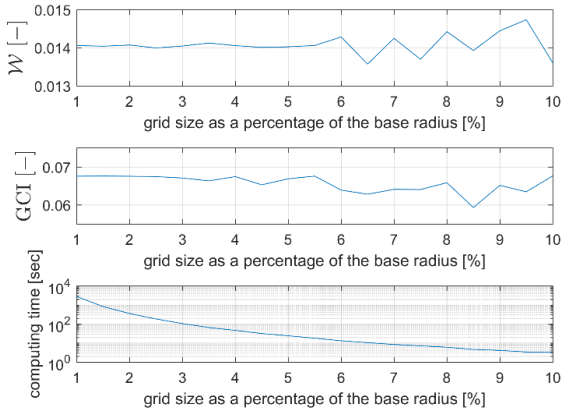

Figure 4. Grid convergence plot.

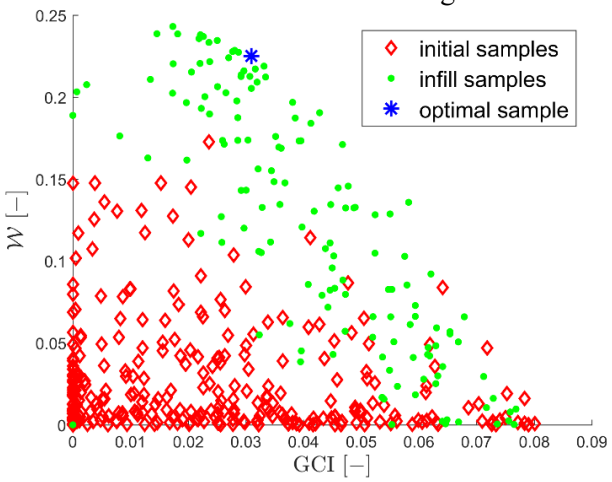

Figure 5. Pareto front on the objective space and the optimal design regarding the weighted-sum function.

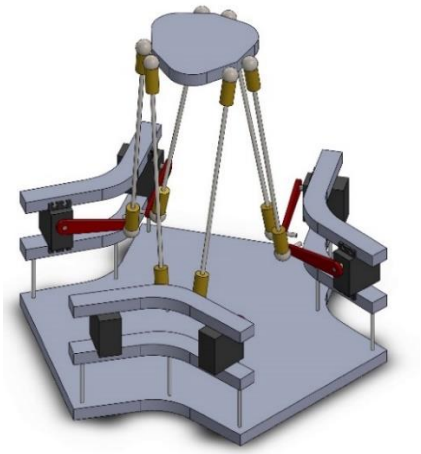

Figure 6. The optimal design of the 6-RSS PM: $l_h = 0.05$ m, $r_b = 0.1$ m, $r_m = 0.042$ m, $z_H = 0.18$ m, $\gamma_b = 25°$, $\gamma_m = 14°$, and $\gamma_h = 153°$.

The SM approach has shown to be highly beneficial in exploring the design landscape thoroughly, even for this case with six design variables. Regarding Figure 5, with just 150 infill points (green dots) the boundary of the objective space was pushed further from the initial data set (red diamonds) to the Pareto front where one objective could not be improved without sacrificing the other objective. On the contrary, directly searching on the true performance functions would not be effective because, for example, the GA search with 100 individuals for 20 generations would require up to 2000 samples to be evaluated with the computationally intensive functions. The presented SM-based approach yielded the optimal manipulator configuration as shown in Figure 6.

6. Conclusions

This paper presented a surrogate-based design method for a 6-RSS PM whose performance was characterised by the volume of the total orientation workspace and the GCI. The existing toolbox was used for generating a space filling sample points as well as for constructing surrogate models of the manipulator performances over a range of design parameter variation. The GA optimiser was then employed to sequentially refine the approximation models and search for the optimal design. Since the surrogate models were relatively less expensive to evaluate when compared to true platform performance evaluation, searching on the approximation models could significantly reduce computational cost in the optimisation process.

The SM approach has been demonstrated to be highly beneficial even for a complex case involving six design variables; it showed to explore the design landscape thoroughly and the Pareto front was identified with just 600 initial samples and 150 infill points. One platform design with the best compromise between the two contradict indices were derived regarding the weighted-sum function.

References

[1] Dasgupta B and Mruthyunjaya T 2000 *Mechanism and Machine Theory* **35** (1) 15–40.
[2] Taghirad H D 2013 *Parallel Robots: Mechanics and Control* (Boca Raton: CRC Press)
[3] Lau T and Zhang Y 2013 New design of 6-RSS parallel manipulator with large rotation workspace *Int. J. Mechanisms and Robot. Syst.* **1** (2/3) 221–239.
[4] Dumlu A and Erenturk K 2013 *Robotica* **32** (04) 643–657
[5] Li K and Wen R 2011 Closed-form dynamic equations of the 6-RSS parallel mechanism through the Newton-Euler approach *Proc. 3rd ICMTMA* **1** 712–715.
[6] Poppeova V, Uricek J, Bulej V and Sindler P 2011 *Technical Gazette* **18** (3) 435–445.
[7] Lou Y, Zhang Y, Huang R, Chen X and Li Z 2014 *IEEE Trans. Autom. Sci. Eng.* **11** (2) 574–584.
[8] Lara-Molina F A, Rosario J M and Dumur D 2010 *The Open Mechanical Eng. J.* **4** (1) 37–47.
[9] Altuzarra O, Pinto C, Sandru B and Hernandez A 2011 *J. Mechanical Design* **133** (4) 041007.
[10] Xie F, Liu X -J and Wang J 2011 Performance evaluation of redundant parallel manipulators assimilating motion/force transmissibility *Int. J. Adv. Robot. Syst.* **8** (5) 113–124.
[11] Patel S and Sobh T 2015 Manipulator performance measures - a comprehensive literature survey *J. Intell. Robot. Syst.* **77** (3-4) 547–570.
[12] Jiang Q and Gosselin C M 2009 Maximal singularity-free total orientation workspace of the GoughStewart platform *J. Mechanisms and Robot.* **1** (3) 034501.
[13] Forrester A I, Sbester A and Keane A J 2008 *Engineering Design via Surrogate Modelling* (Chichester: John Wiley & Sons, Ltd).
[14] Bhosekar A and Ierapetritou M 2018 *Comput. Chem. Eng.* **108** 250–267.
[15] Skinner S N and Zare-Behtash H 2018 *Appl. Soft Comput. J.* **62** 933–962.
[16] Szufnarowski F 2013 Stewart platform with fixed rotary actuators: a low cost design study *Advances in Medical Robotics*
[17] Queipo N V, Haftka R T, Shyy W, Goel T, Vaidyanathan R and Kevin Tucker P 2005 *Progress in Aerosp. Sci.* **41** (1) 1–28.
[18] Xiao S, Rotaru M and Sykulski J K 2012 Exploration versus exploitation using kriging surrogate modelling in electromagnetic design *COMPEL* **31** (5) 1541–1551.
[19] Parr J M, Keane A J, Forrester A I and Holden C M 2012 Infill sampling criteria for surrogate-based optimization with constraint handling *Engineering Optimization* **44** (10) 1147–1166.